

## Article

# NMR and Docking Calculations Reveal Novel Atomistic Selectivity of a Synthetic High-Affinity Free Fatty Acid vs. Free Fatty Acids in Sudlow's Drug Binding Sites in Human Serum Albumin

Themistoklis Venianakis <sup>1</sup>, Alexandra Primikyri <sup>1</sup>, Till Opatz <sup>2</sup> , Stefan Petry <sup>3</sup>, Georgios Papamokos <sup>1,4,\*</sup>  and Ioannis P. Gerothanassis <sup>1,\*</sup> 

<sup>1</sup> Section of Organic Chemistry and Biochemistry, Department of Chemistry, University of Ioannina, GR-45110 Ioannina, Greece; vethemis@gmail.com (T.V.); aleprimik@gmail.com (A.P.)

<sup>2</sup> Department of Chemistry, Johannes Gutenberg-University, Duesbergweg, 10–14, 55128 Mainz, Germany; opatz@uni-mainz.de

<sup>3</sup> Sanofi-Aventis Deutschland GmbH, Integrated Drug Discovery, Industriepark Höchst, 65926 Frankfurt am Main, Germany; stefanmatthias.petry@sanofi.com

<sup>4</sup> Department of Physics, Harvard University, 17 Oxford Street, Cambridge, MA 02138, USA

\* Correspondence: gpapamokos@seas.harvard.edu (G.P.); igeroth@uoi.gr (I.P.G.)

**Abstract:** Saturation transfer difference (STD), inter-ligand NOEs (INPHARMA NMR), and docking calculations are reported for investigating specific binding sites of the high-affinity synthetic 7-nitrobenz-2-oxa-1,3-diazoyl-4-C<sub>12</sub> fatty acid (NBD-C<sub>12</sub> FA) with non-labeled human serum albumin (HSA) and in competition with the drugs warfarin and ibuprofen. A limited number of negative interligand NOEs between NBD-C<sub>12</sub> FA and warfarin were interpreted in terms of a short-range allosteric competitive binding in the wide Sudlow's binding site II (FA7) of NBD-C<sub>12</sub> FA with Ser-202, Lys-199, and Trp-214 and warfarin with Arg-218 and Arg-222. In contrast, the significant number of interligand NOEs between NBD-C<sub>12</sub> FA and ibuprofen were interpreted in terms of a competitive binding mode in Sudlow's binding site I (FA3 and FA4) with Ser-342, Arg-348, Arg-485, Arg-410, and Tyr-411. NBD-C<sub>12</sub> FA has the unique structural properties, compared to short-, medium-, and long-chain saturated and unsaturated natural free fatty acids, of interacting with well-defined structures with amino acids of both the internal and external polar anchor sites in Sudlow's binding site I and with amino acids in both FA3 and FA4 in Sudlow's binding site II. The NBD-C<sub>12</sub> FA, therefore, interacts with novel structural characteristics in the drug binding sites I and II and can be regarded as a prototype molecule for drug development.

**Keywords:** HSA; STD NMR; INPHARMA NMR; docking calculations; NBD-C<sub>12</sub> FA



**Citation:** Venianakis, T.; Primikyri, A.; Opatz, T.; Petry, S.; Papamokos, G.; Gerothanassis, I.P. NMR and Docking Calculations Reveal Novel Atomistic Selectivity of a Synthetic High-Affinity Free Fatty Acid vs. Free Fatty Acids in Sudlow's Drug Binding Sites in Human Serum Albumin. *Molecules* **2023**, *28*, 7991. <https://doi.org/10.3390/molecules28247991>

Academic Editor: Thomas J. Schmidt

Received: 3 November 2023

Revised: 4 December 2023

Accepted: 5 December 2023

Published: 7 December 2023



**Copyright:** © 2023 by the authors. Licensee MDPI, Basel, Switzerland. This article is an open access article distributed under the terms and conditions of the Creative Commons Attribution (CC BY) license (<https://creativecommons.org/licenses/by/4.0/>).

## 1. Introduction

Human serum albumin (HSA) is the most abundant protein in blood plasma, with concentrations of 35–50 g/L and an average half-life of 19 days. It is very stable in a wide range of pH values (4 to 9), withstands temperatures up to 60 °C, and is highly soluble in various organic solvents such as 40% ethanol. HSA maintains oncotic pressure between the blood vessels and tissues; it binds bilirubin, the breakdown product of heme, and many therapeutic drugs such as indole compounds, benzodiazepines, sulfonamides, penicillins, etc. HSA transports a variety of fat-soluble hormones and numerous short-, medium-, and long-chain saturated, mono- and polyunsaturated free fatty acids (FFAs) to the liver and myocytes for energy utilization [1–4]. HSA is a monomeric globular protein of 585 amino acid residues with 17 disulfide bridges. It comprises a single nonglycosylated polypeptide chain with 67%  $\alpha$ -helices without  $\beta$ -sheets. HSA contains three homologous helical domains, I, II, and III, divided into A and B subdomains, forming a heart-shaped molecule.

Pioneering X-ray crystallography studies of Curry et al. [5–8] identified seven binding sites, denoted FA, for a variety of medium- and long-chain mono- and polyunsaturated FFAs. The sites FA1 and FA2 are in the subdomain IB and at the interface between subdomain IA and IIA, respectively. The sites FA3 and FA4 are in the subdomain III A and bind small-molecular-weight aromatic carboxylic acids, such as the drug ibuprofen (Sudlow’s drug binding site II [9], Figure 1). The FA5 is in the subdomain III B, and the FA6 is at the interface between IIA and IIB. The FA7 is in the subdomain IIA and binds heterocyclic negatively charged molecules, such as the drug warfarin (Sudlow’s drug binding site I [9], Figure 1). Two-dimensional  $^1\text{H}$ - $^{13}\text{C}$  HSQC experiments showed the presence of nine binding sites of  $^{13}\text{C}$  methyl-labeled oleic acid bound to HSA [10].

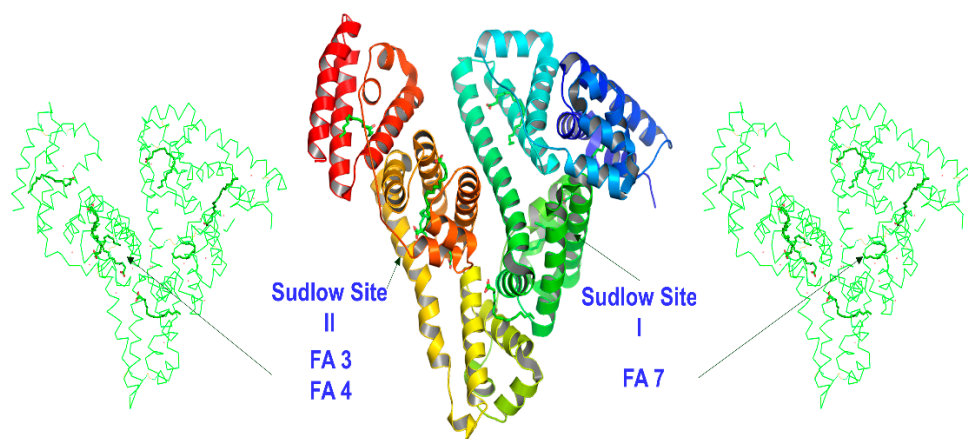


**Figure 1.** HSA Sudlow’s binding sites I and II. The fatty acid binding sites FA3/FA4 and FA7 are indicated on the left and right, respectively.

Competition of drugs with free fatty acids for human albumin Sudlow’s binding sites may significantly affect the potency of drugs [2–4,11,12]. Extensive X-ray structural data of a variety of short- and long-chain saturated, mono- and polyunsaturated FFAs in the binding site FA7 could be modeled only for the methylene trails without determination of the coordination of the carboxylate groups [5–8]. These data were interpreted regarding the low affinity of FFAs; thus, high concentrations of FFAs are required for the efficient displacement of the anticoagulant drug warfarin. Recent STD and INPHARMA NMR as well as docking calculations [13–16] provided a new aspect of molecular recognition of FFAs in FA7. The possibility of two entirely different binding modes of FFAs, due to the presence of two polar amino acid anchor sites, was concluded to be the main reason that the precise coordination of the carboxylic groups could not be obtained by X-ray crystallography.

Recently, a single high-affinity binding site was identified and characterized using the lipophilic derivative 7-nitrobenz-2-oxa-1,3-diazol-4-yl- $\text{C}_{12}$  fatty acid (NBD- $\text{C}_{12}$  FA) [17]. The structure of the HSA molecule is more similar to the fat-free structure (2.8 Å rmsd [18]) than the HSA structure with seven bound fatty acids (5.3 Å rmsd [6]). It was concluded, on the basis of X-ray and fluorescence experiments [17], that the binding site of the NBD- $\text{C}_{12}$  FA conjugate is not identical with the warfarin binding site in HSA; however, it partly overlaps with the latter. A lower electron density near the side chain of Tyr-411, which is a critical amino acid residue for the binding of the drug ibuprofen, was also observed [17]. Fitting a second molecule of NBD- $\text{C}_{12}$  FA resulted in strong electron density of the 4-nitrobenzoxadiazole group; however, the intensity of the fatty acid part of the molecule was very weak.

Understanding, at the atomic level, the selectivity of high-affinity ligands for HSA, such as the lipophilic fatty acid derivative NBD- $\text{C}_{12}$  FA, is very important for drug discovery since they can compete effectively with free fatty acids for HSA Sudlow’s binding sites. We therefore report herein combined NMR (saturation transfer difference-STD) [13–16,19–21], 2D-Tr NOESY [22–24], and interligand NOEs for pharmacophore mapping (INPHARMA) [13–16,25–27]) as well as

docking calculations [28–31] of the high-affinity ligand NBD-C<sub>12</sub> FA in competition experiments with two drugs: warfarin, which is a stereotypical anticoagulant drug for FA7, and ibuprofen, which is an anti-inflammatory drug for FAs 3 and 4. A unified atomic level model for the selectivity of NBD-C<sub>12</sub> FA vs. short-, medium-, and long-chain mono- and polyunsaturated FFAs is proposed.

## 2. Results and Discussion

### 2.1. STD and INPHARMA NMR Competition Experiments of NBD-C<sub>12</sub> FA with Warfarin and Ibuprofen

#### 2.1.1. The FA7 Binding Site

The <sup>1</sup>H NMR spectrum of warfarin (W) (2 mM) with HSA (25 μM) is shown in Figure 2a. Despite the addition of an equimolar quantity of NBD-C<sub>12</sub> (2 mM), the relative integrals of the H5(W) and H6'(NBD-C<sub>12</sub>) protons showed a molar ratio of W/NBD-C<sub>12</sub>~2/1, presumably due to very low solubility of the fatty acid analogue. Despite the low concentration of NBD-C<sub>12</sub>, a reduction in the linewidths of warfarin was observed, especially those of the aromatic H7 and the strongly overlapped H3', 5', 6, 8, and H4'. In addition, the linewidth of the H6' and H5' of NBD-C<sub>12</sub> ( $\Delta\nu_{1/2} \approx 20$  Hz) is significantly larger than that of, e.g., the H5 of warfarin (doublet with  $\Delta\nu_{1/2} \approx 5$  Hz). Similar results were obtained with the STD NMR experiments. The STD NMR spectrum of warfarin in the presence of HSA shows strong resonances of the aromatic protons (Figure 2b). The epitope mapping of the protons of the bound warfarin was evaluated with the determination of the STD amplification factor ( $A_{STD}$ ), which reflects the proximity of the protons to the binding site on HSA. The STD signals were normalized with respect to the signal with the highest  $A_{STD}$  values, which was set to 100%. All the protons show  $A_{STD}$  values above 37%, which shows the efficient binding of warfarin to HSA. The STD line widths and intensities of warfarin bound to HSA upon adding NBD-C<sub>12</sub> FA are reduced (Figure 2d), especially those of the H7, H3', 5', 6, 8, and H4', with a reduction of the  $A_{STD}$  values in the range of 5 to 37% (Figure 2).

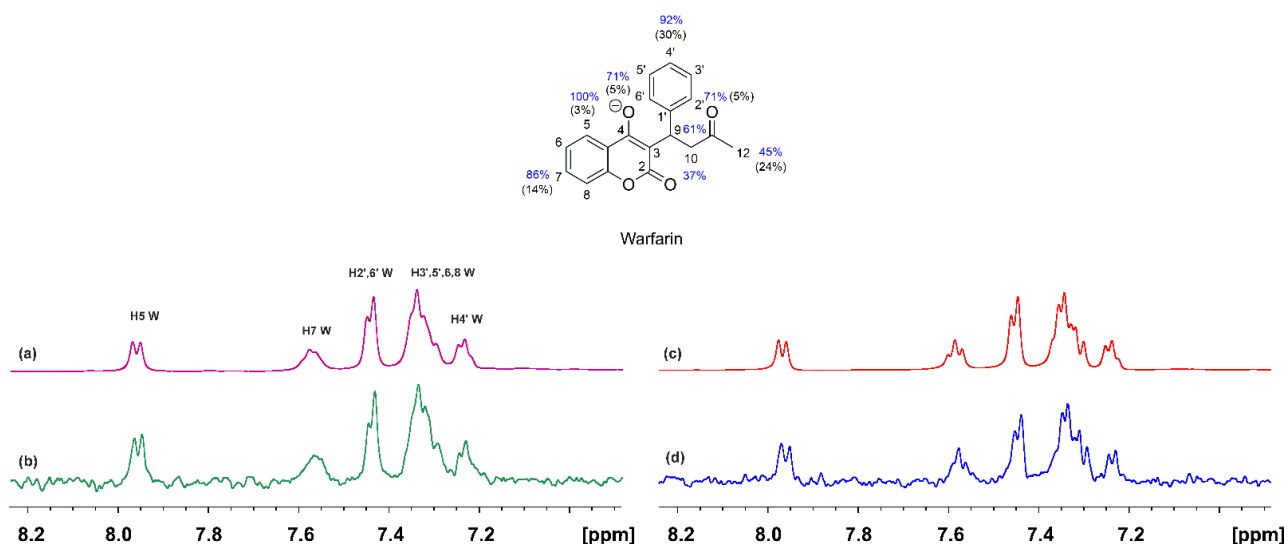


**Figure 2.** <sup>1</sup>H NMR spectra (500 MHz) of (a) warfarin (W) (2 mM) with native HSA (25 μM) in 50 mM PBS buffer in D<sub>2</sub>O with 20% DMSO-d<sub>6</sub> (T = 323 K); (c) as in (a) after the addition of 2 mM of NBD-C<sub>12</sub> FA; (b) STD <sup>1</sup>H NMR spectrum of (a). (d) STD <sup>1</sup>H NMR spectrum of (c). The STD amplification factor of warfarin in the binary HSA warfarin complex is shown in blue color and the % reduction upon addition of NBD-C<sub>12</sub> FA is shown in black.

Extensive complexation studies of warfarin with HSA showed a wide range of formation constants ( $\sim 1.4 \times 10^6$ – $2.3 \times 10^3$  M<sup>-1</sup>) depending on the experimental techniques and conditions used [32–35]. A formation constant of  $\sim 2 \times 10^5$  M<sup>-1</sup> was determined for

warfarin by the switch sense method, which can be compared with the values for the NBD-C<sub>12</sub> FA of  $\sim 0.37 \times 10^5 \text{ M}^{-1}$  by fluorescence titration and the switch sense method and  $\sim 0.68 \times 10^5 \text{ M}^{-1}$  by dialysis [17].

The above NMR competition experimental data can be analyzed in terms of: (i) two ligands which are competitive towards the FA7 binding site; (ii) short-range (<5 Å) allosteric interaction in the wide FA7 site; and (iii) long-range (>5 Å) allosteric interaction which results in conformational changes in FA7 and, thus, a decrease in the affinity of warfarin.

The use of the 2D Tr-NOESY (INPHARMA) NMR technique [25,26], which is based on observing inter-NOEs between two ligands that bind competitively to a common binding site with distances < 5 Å, can be utilized to resolve the above ambiguity. The competition experiment of NBD-C<sub>12</sub> FA with warfarin (Figure 3) shows the presence of a limited number of inter-NOEs (denoted with the red cross-peaks) between the H2', 6', and H4' protons of the phenyl ring of warfarin and the H4-9 protons of NBD-C<sub>12</sub> FA, which are close in space (<5 Å). Of particular interest is the absence of common inter-NOEs between the aromatic protons of the two ligands, which demonstrates that the phenyl butyl and benzopyran ring of warfarin and the 7-nitrobenz-2-oxa-1,3-diazol-4-yl moiety of NBD-C<sub>12</sub> FA are at distances > 5 Å, i.e., beyond the detection limits of NOE experiments. Cross-peaks between the two ligands in the absence of HSA were not observed. This demonstrates that the interligand NOEs of Figure 3 result from a spin-diffusion process through the HSA protons due to the partial proximity of the phenyl group of warfarin and the 4–9 protons of NBD-C<sub>12</sub> FA in the binding site FA7. Nevertheless, the presence of a limited number of inter-NOE connectivities between NBD-C<sub>12</sub> FA and warfarin is contrary to the significant number of negative 2D interligand NOEs that were observed between short (caproic), medium (oleic, linoleic, and  $\alpha$ -linolenic acids) and long (EPA and DHA) FFAs and warfarin [13–16], which demonstrates a common binding mode in FA7 and the presence of two polar amino acid anchor sites (see discussion on docking calculations).

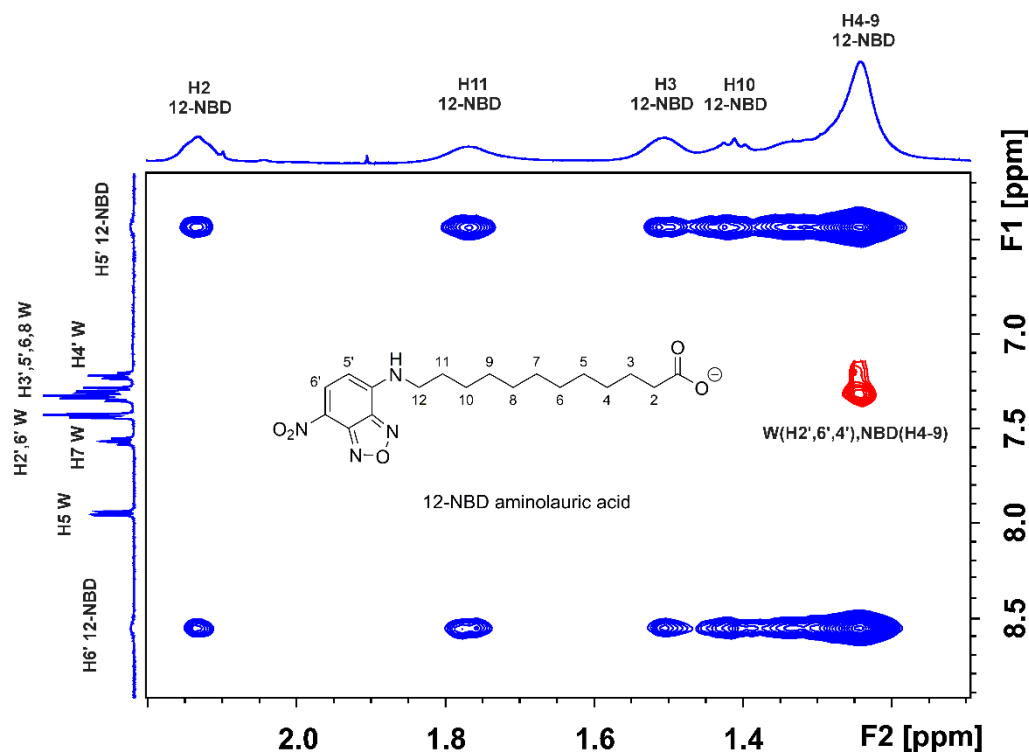


**Figure 3.** Interligand 2D Tr-NOESY (INPHARMA) NMR spectrum (500 MHz) of NBD-C<sub>12</sub> FA (0.8 mM saturated solution) in the presence of warfarin (W) (1.6 mM) with native HSA (25  $\mu\text{M}$ ) in 50 mM PBS buffer in D<sub>2</sub>O with 20% DMSO-d<sub>6</sub>, T = 323 K, mixing time = 300 ms. The red cross-peaks denote interligand NOEs between NBD-C<sub>12</sub> FA and warfarin.

### 2.1.2. The FA3 and FA4 Binding Sites

The  $^1\text{H}$  NMR spectrum of ibuprofen in complexation with HSA is shown in Figure 4a. Despite the addition of NBD- $\text{C}_{12}$  FA at a molar ratio of 1/1, the resulting relative integrals of the H5,9 (IB) and H6' (NBD- $\text{C}_{12}$  FA) showed a molar ratio of IB/NBD- $\text{C}_{12}$  FA~2/1 to 4/1 due to low solubility of the synthetic analogue. Despite the significantly smaller concentration of NBD- $\text{C}_{12}$  FA, a reduction in the linewidth of ibuprofen is observed (Figure 4c), which probably reflects competition towards the same binding site. A similar conclusion can be drawn from the STD experiments (Figure 4b,d). Again, the epitope mapping of the protons of the bound ibuprofen was evaluated with the determination of the STD amplification factor ( $A_{\text{STD}}$ ). All the protons show  $A_{\text{STD}}$  values above 62%, which shows the efficient binding of ibuprofen with HSA. Addition of NBD- $\text{C}_{12}$  FA shows a reduction of the  $A_{\text{STD}}$  values in the range of 14 to 17%. Nevertheless, to assess whether the reduction in the line widths and amplitude of the STD signals reflects competitive interactions towards the FA3 and FA4 binding sites or, rather, that NBD- $\text{C}_{12}$  FA binds at a different site and results in long-range conformational changes in FA3/FA4 (long-range allosteric inhibition), the 2D-Tr NOESY (INPHARMA) NMR method was applied.

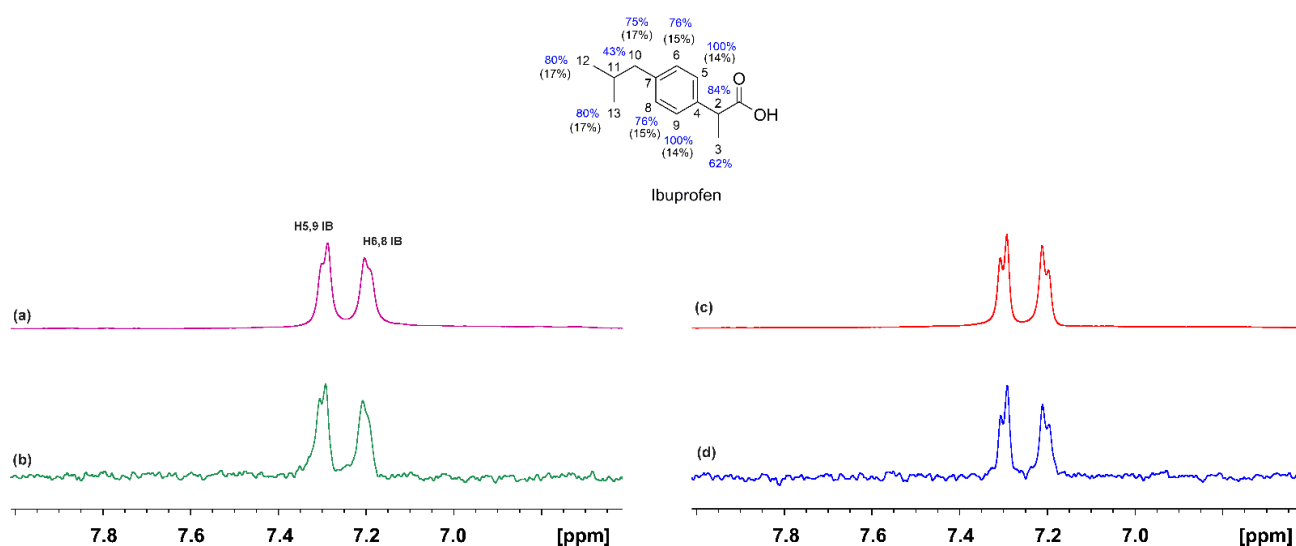


**Figure 4.**  $^1\text{H}$  NMR spectra (500 MHz) of: (a) ibuprofen (I) (2 mM) with native HSA (25  $\mu\text{M}$ ) in 50 mM PBS buffer in  $\text{D}_2\text{O}$  with 20%  $\text{DMSO-d}_6$  ( $T = 323\text{ K}$ ); (c) as in (a) after the addition of 2 mM of NBD- $\text{C}_{12}$  FA; (b) STD  $^1\text{H}$  NMR spectrum of (a). (d) STD  $^1\text{H}$  NMR spectrum of (c). The STD amplification factor of ibuprofen in the binary HSA ibuprofen complex is shown in blue color and the % reduction upon the addition of NBD- $\text{C}_{12}$  FA is shown in black.

Figure 5 shows the 2D Tr-NOESY (INPHARMA) NMR competition experiment of NBD- $\text{C}_{12}$  FA and ibuprofen which indicates the presence of very characteristic negative inter-NOEs (denoted with the red cross-peaks; in-phase with respect to those of the diagonal) between H5,9 and H6,8 of ibuprofen with the H2, H3, and H4–9 of NBD- $\text{C}_{12}$  FA. Significant interligand NOE connectivities were also observed between H2 of ibuprofen with H3 and H2 of NBD- $\text{C}_{12}$  FA. Similar results were obtained with 2D Tr-NOESY (INPHARMA) NMR competition experiments of NBD- $\text{C}_{12}$  FA (400  $\mu\text{M}$ ) and ibuprofen (400  $\mu\text{M}$ ) using mixing times of 300 ms and 200 ms (Figure S1). This finding confirms NOE transfer between the two ligands with distances  $< 5\text{ \AA}$  and, thus, competition towards a common binding site. Cross-peaks between the two ligands in the absence of HSA were not observed (Figure S2), which demonstrates that the interligand NOEs of Figure 5 are not due to the direct transfer of magnetization between ibuprofen and NBD- $\text{C}_{12}$  FA; they are mediated from a spin-diffusion process through the HSA protons.

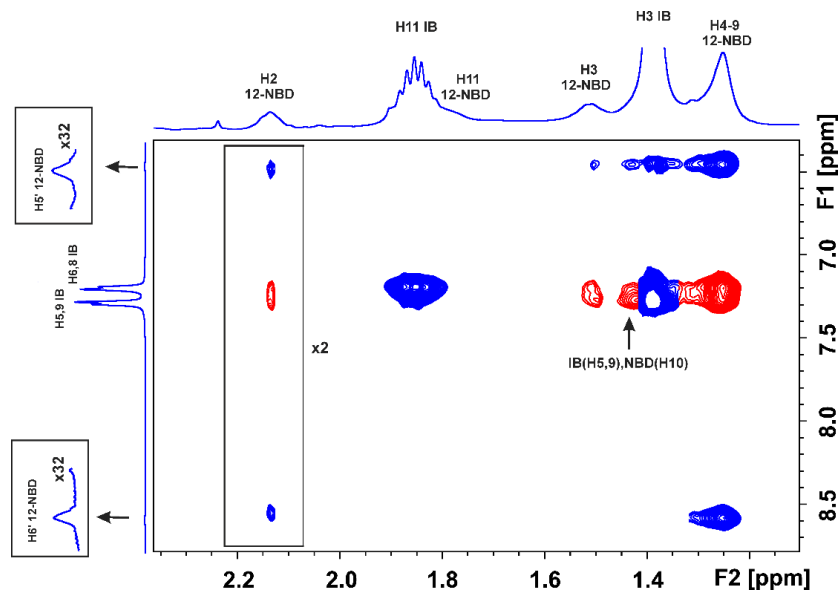


**Figure 5.** Interligand 2D Tr-NOESY (INPHARMA) NMR spectrum (500 MHz) of NBD- $C_{12}$  FA (0.8 mM saturated solution) in the presence of ibuprofen (IB) (1.6 mM) with native HSA (25  $\mu$ M) in 50 mM PBS buffer in  $D_2O$  with 20%  $DMSO-d_6$ ,  $T = 323$  K, mixing time = 300 ms. Interligand NOEs between NBD- $C_{12}$  FA and ibuprofen are denoted with the red cross-peaks (x is a multiplication factor).

## 2.2. Docking Calculations

Molecular docking is a valuable method in drug design. Thus, millions of molecules of known structures retrieved from virtual libraries are tested against drug targets using high-performance computers and high-scalability software tools [36]. Nonetheless, several deficiencies have been reported in the past [37,38], and various solutions have been proposed to overcome the limits of the accuracy of this method [39,40]. Recent developments include newly established techniques such as deep learning [41] that may address the known problem of irreproducibility in biomedical research [42].

In our previous studies, we have used an approach based on site-specific docking, guided by experimental results of NMR and X-ray crystallography, which has proven very successful in locating poses consistent with experimental results [13,15,27]. The question set by the experimental results of NMR and the X-ray crystallography is the structural arrangement of the drugs warfarin (W) at the binding site FA7 and ibuprofen (IB) at binding sites FA3 and FA4. The preferred structural arrangement, according to the experimental results generated by the above techniques, must fulfill the following spatial requirements:

1. The (7-nitrobenz-2-oxa-1,3-diazol-4-yl)- $C_{12}$  fatty acid [17] and the drug warfarin interact weakly through the FA's methylene groups and the drug's phenyl butyl moiety in the binding site FA7.
2. The NBD- $C_{12}$  fatty acid interacts with the drug ibuprofen in the binding sites FA3 and FA4.

### 2.2.1. The FA7 Binding Site

The FA7 binding site, although primarily hydrophobic, contains two clusters of polar amino acids: an internal one with amino acids Tyr-150, His-242, and Arg-257 and an external one, in the entrance of the pocket, with amino acids Lys-195, His-242, Arg-218, and Arg-222 [8,43]. Initially, we performed site-specific warfarin docking in the presence of NBD- $C_{12}$  FA (pdb code: 6eqz.pdb). To be consistent with the above NMR results, we varied the grid and the box's center accordingly and selected the poses that agreed with the experiment. The docking results indicate that warfarin interacts with amino acids Arg-218 and Arg-222 of the external cluster. The binding also includes Lys-195 and Asp-451. The docking calculations showed that carbon No 10 (C10) of the NBD- $C_{12}$  FA is close to the single aromatic ring (3.9 Å). These results are presented in Table 1 and Figure 6A–D.

**Table 1.** Results from docking calculations. Electrostatic and hydrogen bond interactions in the binding site FA7 of HSA, successful pose, and affinities in kcal/mol. <sup>1</sup>. Docking of warfarin in the presence of NBD-C<sub>12</sub> FA (crystal structure employed: 6EZQ.pdb) <sup>2</sup>. Docking of NBD-C<sub>12</sub> FA in the presence of warfarin (crystal structure: 2BXD.pdb).

	HSA/Amino Acid Group	Dist. (Å)	Pose /Predicted Affinity (kcal/mol)
1. Atom-No of Warfarin			
-	K-199		
O <sub>15</sub>	R-218/NH <sub>2</sub> η <sup>1</sup>	3.0	6/−5.5
O <sub>15</sub>	R-222/NH <sub>2</sub> η <sup>2</sup>	3.1	
O <sub>13</sub>	D-451/OD2	3.3	
C <sub>4</sub> '	K-195/N ζ	3.6	
C <sub>3</sub> '	NBD/C <sub>10</sub>	3.9	
2. Group or Atom-No of NBD-C <sub>12</sub> FA			
COO <sup>−</sup>	K-199	2.1	6/−6.5
COO <sup>−</sup>	R-222	3.4	
COO <sup>−</sup>	R-218	4.0	
Aromatic ring-C <sub>2</sub> '	W-214	3.5	
NH	S-202	1.9	

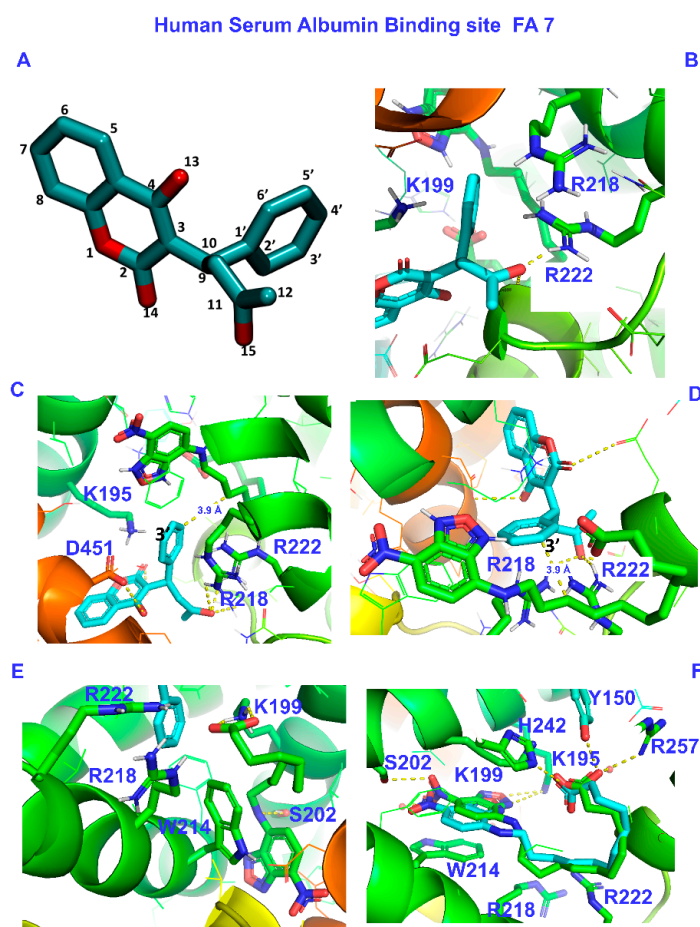


**Figure 6.** (A) Atom-numbering of warfarin molecule. (B–D). Different views of successful docking pose of warfarin in the presence of NBD-C<sub>12</sub>-FA. (E) Successful docking pose of NBD-C<sub>12</sub>-FA in the presence of warfarin. (F) Self-docking of NBD-C<sub>12</sub>-FA and superposition with the crystal structure.

In a subsequent step, we repeated the site-specific docking (FA7), for NBD-C<sub>12</sub> FA, in the presence of warfarin (crystal structure pdb code: 2BXD.pdb). The results are shown in Table 1 and Figure 6E. The carboxylate group interacts with Lys 199, Arg-218, and Arg-222 of the external cluster. The nitro group terminal side interacts with Ser-202 through the NH group, and there is a pi-pi stacking interaction between the aromatic rings of NBD and Trp-214.

Additionally, we performed site-specific docking to verify the accuracy of our approach. Consequently, we removed NBD-C<sub>12</sub> FA from its crystal structure (6EZQ.pdb) and used the free protein and NBD-C<sub>12</sub> FA as ligands (self-docking). The binding, depicted by X-ray, was reproduced with our docking calculations: The nitro group interacts with Ser-202 and Trp-214, and the carboxylate group at FA7 interacts with Lys-199 and His-242. The docking calculations revealed that Tyr-150, Lys-195, and Arg-257 may also be involved in the binding (see Figure 6F below and Figure 3A in reference [17]).

From the results of this work, it is evident that warfarin occupies the remaining space of FA7 left free by the NBD-C<sub>12</sub> FA, which is in line with previous observations from fluorescence titration experiments [17]. Although the interaction of warfarin with residues Arg-218 and Arg-222 is expected from X-ray [8] and our docking calculations [13], the Lys-195 residue seems to alter the interaction in the FA7.

The crystal structure of HSA-NBD-C<sub>12</sub> FA (6EZQ) shows that the nitro group interacts with Ser-202 and Trp-214, and the carboxylate group interacts with Lys-199 and His-242 (see also Figure 3A in reference [17]). Moreover, upon binding of warfarin, a spatial rearrangement is observed for HSA, which has also been noticed before [9,44]. The authors showed that warfarin and NBD-C<sub>12</sub> FA binding does not constitute a competitive mechanism [17]. Our docking results, which meet the demands of the crystal structure and NMR findings, indicate a non-competitive (allosteric) binding of warfarin at FA7, which can also alter this binding site. Additionally, to account for the fluorescence results [17], we performed flexible docking calculations of warfarin in the presence of the NBD-C<sub>12</sub> FA ligand. The resulting orientations of the flexible aromatic rings of NBD-C<sub>12</sub> FA and Trp-214 remained essentially the same. A slight change in the relative arrangement of the NBD moiety and Trp-214 or the repulsion of a molecule of water from the cavity can result in an increased NBD fluorescence.

### 2.2.2. The FA3 and FA4 Binding Sites

Our docking results show that the NBD-C<sub>12</sub> FA occupies the FA3 entirely through interactions of the carboxylate group with Ser-342, Arg-348, and Arg-485. The nitro group interacts with Arg-410 and Tyr-411 in one of the anchoring sites of FA4 (cluster 1, Table 2), which is more elongated and narrow than the site FA3. These interactions are similar to those based on the X-ray electron density and on fluorescence data [17]. A binding site of ibuprofen in FA3 was previously identified by docking calculations [13] which also involve Ser-342, Arg-348, and Arg-485 (Table 3). This is in agreement with the common interligand NOE connectivities of H2 of ibuprofen with H3 and H2 of NBD-C<sub>12</sub> FA ligand.

**Table 2.** Comparison of electrostatic and hydrogen bond interactions of DHA, EPA, ALA, NBD-C<sub>12</sub> FA, and warfarin in the two anchor sites of FA7.

Ligand	FA7	
	Inner Cluster	External Cluster
	Tyr-150, His-242, Arg-257	Lys-195, Lys-199, Arg-218, Arg-222
DHA (docking) <sup>a</sup>	His-242, Arg-257 (−7.0 kcal/mol)	Lys-199, Arg-218, Arg-222 (−7.0 kcal/mol)
EPA (docking) <sup>a</sup>	His-242, Arg-257 (−6.7 kcal/mol)	Lys-199, Arg-218, Arg-222 (−6.8 kcal/mol)

Table 2. Cont.

Ligand	FA7	
	Inner Cluster	External Cluster
Warfarin (docking) <sup>b</sup>	His-242, Arg-257 (−7.0 kcal/mol)	Arg-218, Arg-222 (−7.7 kcal/mol)
NBD-C <sub>12</sub> (X-ray)	His-242, Ser-202 NO <sub>2</sub>	Lys-199, Trp-214 COO <sup>−</sup>
NBD-C <sub>12</sub> (docking)	His-242, Ser-202 NO <sub>2</sub>	Lys-199, Trp-214 COO <sup>−</sup>
Warfarin in the presence of NBD-C <sub>12</sub> (docking)	-	(−7.3 kcal/mol) Lys-195, Arg-218, Arg-222 (−5.5 kcal/mol)
NBD-C <sub>12</sub> in the presence of warfarin (docking)	Ser-202, Trp-214 NO <sub>2</sub>	Lys-199, Arg-218, Arg-222 COO <sup>−</sup>
		(−6.5 kcal/mol)

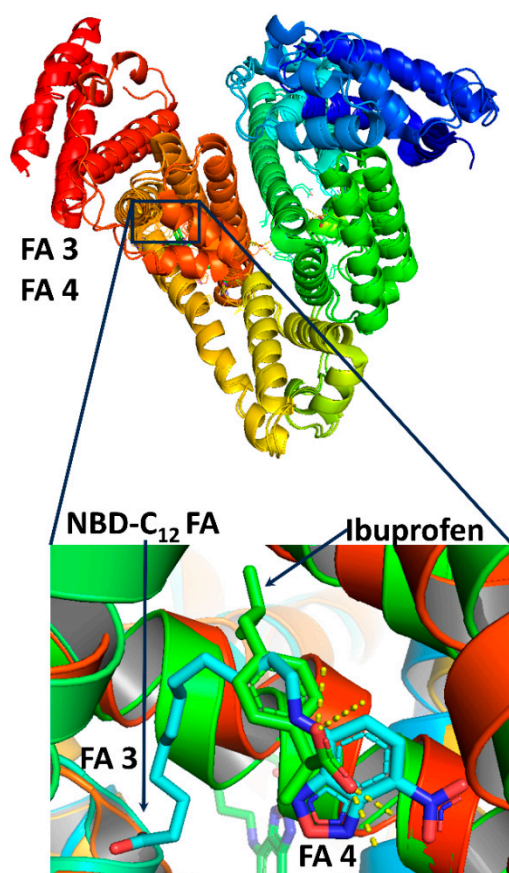
<sup>a</sup> Ref. [15], <sup>b</sup> Ref. [13].

Table 3. Comparison of electrostatic and hydrogen bond interactions of ALA, DHA, NBD-C<sub>12</sub> FA, and ibuprofen in the anchor sites of FA3 and FA4.

	FA3	FA4	
		Cluster-1	Cluster-2
DHA (docking) <sup>a</sup>	Ser-342, Arg-348, Arg-485 (−8.3 kcal/mol)	Arg-410, Tyr-411 (−7.5 kcal/mol)	Ser-419, Thr-422 (−7.8 kcal/mol)
EPA (docking) <sup>a</sup>	Ser-342, Arg-348, Arg-485 (−7.9 kcal/mol)	Arg-410, Tyr-411 (−7.0 kcal/mol)	Ser-419, Thr-422 (−7.8 kcal/mol)
Ibuprofen (docking) <sup>b</sup>	Ser-342, Arg-348, Arg-485 (−7.2 kcal/mol)	Arg-410, Tyr-411 (−7.3 kcal/mol)	
Ibuprofen (X-ray)		Arg-410, Tyr-411	
NBD-C <sub>12</sub> (X-ray)	Ser-342, Arg-348, Arg-485 COO <sup>−</sup>	Arg-410, Tyr-411 NO <sub>2</sub>	
NBD-C <sub>12</sub> (docking)	Ser-342, Arg-348, Arg-485 COO <sup>−</sup>	Arg-410, Tyr-411 NO <sub>2</sub>	
		(−8.3 kcal/mol)	
Ibuprofen in the presence of NBD-C <sub>12</sub> (docking)	-	-	

<sup>a</sup> Ref. [15], <sup>b</sup> Ref. [13].

Repeated docking simulations of ibuprofen in the presence of NBD-C<sub>12</sub> FA systematically failed to bind in FA3 since the carboxyl group of the NBD-C<sub>12</sub> FA does not allow such interaction. Ibuprofen binding is possible only when this interacts with the anchoring site comprised of Arg-410 and Ser-411, which is identical to NBD-C<sub>12</sub> FA. Docking calculations for ibuprofen in FA4 indicate that interaction occurs out of the protein cage, entailing a lack of binding. Based on our NMR experiments and the conclusion of Wenskowsky et al. [17] that ibuprofen shows no appreciable effect at the relatively low concentrations in their fluorescence assay, we conclude that (a) for the NBD-C<sub>12</sub> FA, the FA7 is the primary binding site and (b) the significantly higher concentration of ibuprofen relative to that of NBD-C<sub>12</sub> FA resulted in observable antagonistic phenomena in our STD and 2D Tr-NOESY experiments. Figure 7 shows a superposition of NBD-C<sub>12</sub> FA and ibuprofen in FA3/FA4 binding sites, in excellent agreement with our 2D Tr-NOESY experiments.



**Figure 7.** Superposition of NBD-C<sub>12</sub> FA and ibuprofen in FA3/FA4 binding sites (crystal structure codes in PBB: 6ezq.pdb and 2bxg.pdb).

### 2.3. A Unified Atomic Level for the Selectivity of NBD-C<sub>12</sub> FA and Short, Medium, and Long Mono- and Polyunsaturated Free Fatty Acids

We have recently demonstrated the presence of two orientations of mono- and polyunsaturated FFAs in the warfarin binding site FA7 due to the presence of two potential polar anchor sites: an inner cluster composed of the amino acids Tyr-150, His-242, and Arg-257 and an external cluster of the amino acids Lys-195, Lys-199, Arg-218, and Arg-222 [13,15,16]. Interestingly, increasing the length and polyunsaturation of the chain increases the affinity of FFAs due to hydrophobic interactions and the ability to adopt folded conformations [15]. The NBD-C<sub>12</sub> FA binding mode in FA7 in the presence of warfarin is unique since the carboxylate group binds to amino acids in the external cluster (Lys-199, Arg-218, and Arg-222, Table 2). The NO<sub>2</sub> group binds to amino acids in the inner cluster (Ser-202 and Trp-214, Table 2), which significantly reorganizes this binding site. Binding of NBD-C<sub>12</sub> FA, therefore, modifies the FA7 binding site without changing the overall structure. The significant remaining space allows the binding of warfarin in the external cluster with limited contacts with the NBD-C<sub>12</sub> FA molecule.

The binding mode of the carboxylate group of NBD-C<sub>12</sub> FA in FA3 is identical to that of DHA and EPA and involves interactions with Ser-342, Arg-348, and Arg-485 (Table 3). The NO<sub>2</sub> group interacts with Arg-410 and Tyr-411 of cluster 1 in FA4, which results in significant high affinity. The remaining space of cluster 2 of FA4 is insufficient for the accommodation and interaction with ibuprofen.

## 3. Material and Methods

### 3.1. Chemicals and Reagents

Warfarin and ibuprofen, purity  $\geq 98\%$  (GC), and human serum albumin fatty acid-depleted lyophilized powder, purity  $\geq 96\%$  (agarose gel electrophoresis), were obtained

from Sigma Aldrich Chemie, GmbH, Taufkirchen, Germany. D<sub>2</sub>O and DMSO-d<sub>6</sub> (>99.8%) were obtained from Deutero GmbH, Kastellaun, Germany. The NBD-C<sub>12</sub> FA was synthesized according to [17].

### 3.2. NMR Experiments

STD and 2D Tr-NOESY (INPHARMA) NMR experiments were performed on a Bruker AV-NEO-500 spectrometer in the presence of HSA (25 μM) and 50 mM PBS (pD = 7.4) in D<sub>2</sub>O with 20% DMSO-d<sub>6</sub> at 323 K to facilitate the dissolution of NBD-C<sub>12</sub> FA. STD experiments were performed with selective saturation of 2 s with a train of Gaussian-shaped pulses, as previously reported [15,16,27]. Two-dimensional Tr-NOESY (INPHARMA) experiments were recorded with 80 scans, 2 K data block with 110 incremental values of the revolution times, and total experiment time ~15 h.

### 3.3. Computational Methods

Details of the computational approach are discussed in Refs [13,15,39]; herein, a summary is provided. The crystal structure of the complex of human serum albumin (HSA) with the ligand (7-nitrobenz-2-oxa-1,3-diazol-4-yl)-C<sub>12</sub> (NBD-C<sub>12</sub>) FA was obtained from the Protein Data Bank. The entry code name is 6EZQ. Since experimental data indicate the coexistence of NBD-C<sub>12</sub> FA and warfarin or ibuprofen at the binding sites 3–4 and 7, we did not remove the NBD-C<sub>12</sub> FA from the initial structure. In contrast, we attempted site-specific docking with NBD-C<sub>12</sub> present and defining a search space consistent with the known amino acids responsible for the binding of warfarin and ibuprofen, excluding those that the NBD-C<sub>12</sub> FA occupies. The AutoDock Vina1.1.2 [30] software package was employed for the docking calculations. The AutoDock Tools 1.5.6 software package [29] was used as a preprocessing software package to add hydrogen atoms to the protein and select the search space for each complex studied. The selection of the poses was based on (a) inter-residue NOE intensities in competition experiments, (b) the highest affinity (10 independent runs for each binding site), and (c) minimum deviation from the X-ray crystal structure. Configuration files of docking are provided in Supplementary Materials.

## 4. Conclusions

The present work highlights the great potential of the combined use of 2D Tr-NOESY (INPHARMA) NMR and computational methods [13,15,16,26,27,45] to investigate structural and functional aspects of ligand–macromolecule interactions. More specifically:

- The limited number of negative interligand NOEs between H4–9 protons of NBD-C<sub>12</sub> FA and protons of the phenyl ring of warfarin and the absence of common inter-NOEs between the aromatic rings of the two ligands were interpreted in terms of a short-range negative allosteric competitive binding of NBD-C<sub>12</sub> FA with the amino acids Ser-202, Lys-199, Trp-214, and warfarin with Arg-218 and Tyr-411 in the wide binding site FA7.
- The extensive number of interligand NOEs between H2, H3, and H4–9 of NBD-C<sub>12</sub> FA and the aromatic protons H5,9 and H6,8 of ibuprofen was interpreted in terms of a competitive binding mode with Ser-342, Arg-348, Arg-485, Arg-410, and Tyr-411 in the binding sites FA3 and FA4.
- The self-docking protocol of the ligands NBD-C<sub>12</sub> FA, warfarin, and ibuprofen on the X-ray HSA–ligand structure allowed us to define the search space as precisely as possible and, thus, accurately define electrostatic and hydrogen bond interactions between ligands and HSA.
- Compared to short-, medium-, and long-chain mono- and polyunsaturated FFAs, the NBD-C<sub>12</sub> FA has the unique structural characteristics of interacting with amino acids of both the internal and external clusters in Sudlow's binding site I. In Sudlow's binding site II, the NBD-C<sub>12</sub> FA interacts with amino acids in both FA3 and FA4.
- X-ray and NMR-based docking calculations with site-specific docking has been proven to constitute a very successful method to elucidate and describe the generated elec-

trostatic and H-bonded interactions between the ligands and the HSA protein at an atomic level.

The NBD-C<sub>12</sub> FA, therefore, results in a significant reorganization in Sudlow's drug binding sites and, thus, could be important for drug depot development and improved pharmacokinetics. Further studies are currently underway to investigate polyunsaturated FFAs conjugates with drugs to further understand drug–HSA binding modes.

**Supplementary Materials:** The following supporting information can be downloaded at <https://www.mdpi.com/article/10.3390/molecules28247991/s1>: Figure S1: Interligand 2D Tr-NOESY (IN-PHARMA) NMR spectrum (500 MHz) of NBD-C<sub>12</sub> FA (400 μM) in the presence of ibuprofen (I) (400 μM) with native HSA (25 μM) in 50 mM PBS buffer in D<sub>2</sub>O with 20% DMSO-d<sub>6</sub>, T = 323 K, mixing time = 200 ms. Interligand NOEs between NBD-C<sub>12</sub> FA and ibuprofen are denoted with the red cross-peaks. Figure S2: Interligand 2D Tr-NOESY NMR spectrum of NBD-C<sub>12</sub> FA (0.8 mM, saturated solution) and ibuprofen (IB) (1.6 mM) in 50 mM PBS buffer in D<sub>2</sub>O with 20% DMSO-d<sub>6</sub>, T = 323 K, mixing time = 300 ms. The H6' and H5' cross-peaks of NBD-C<sub>12</sub> FA and H5,9 and H6,8 of ibuprofen are anti-phase with respect to the diagonal due to fast molecular tumbling of the ligands within the extreme narrowing condition. Configuration files of docking calculations: warfarin–HSA docking in the presence of NBD-C<sub>12</sub>; NBD-C<sub>12</sub>–HSA docking in the presence of warfarin; NBD-C<sub>12</sub>–HSA docking in free HSA.

**Author Contributions:** Conceptualization, G.P. and I.P.G.; NMR experiments, T.V. and A.P.; computations, G.P.; methodology, T.O., S.P., T.V., G.P. and I.P.G.; funding acquisition and project administration, I.P.G. All authors have read and agreed to the published version of the manuscript.

**Funding:** The Hellenic Foundation for Research and Innovation (H.F.R.I.) under the “First Call for H.F.R.I. Research Projects to support Faculty members and Researchers and the procurement of high-cost research equipment grant” (Project Number: 2050) is gratefully acknowledged for financial support.

**Institutional Review Board Statement:** Not applicable.

**Informed Consent Statement:** Not applicable.

**Data Availability Statement:** Data are contained within the article and Supplementary Materials.

**Conflicts of Interest:** S.P. is an employee and shareholder of Sanofi. The other authors declare no conflict of interest.

## References

1. Hodgson, J. *All about Albumin: Biochemistry, Genetics and Medical Applications*; Academic Press: San Diego, CA, USA, 2001.
2. Wenskowsky, L.; Wagner, M.; Reusch, J.; Schreuder, H.; Matter, H.; Opatz, T.; Petry, M.S. Resolving binding events on the multifunctional human serum albumin. *Chem. Med. Chem.* **2020**, *15*, 738–743. [[CrossRef](#)] [[PubMed](#)]
3. Mishra, V.; Heath, R.J. Structural and biochemical features of human serum albumin essential for eukaryotic cell culture. *Int. J. Mol. Sci.* **2021**, *22*, 8411. [[CrossRef](#)] [[PubMed](#)]
4. Di Massi, A. Human serum albumin: From molecular aspects to biotechnological applications. *Int. J. Mol. Sci.* **2023**, *24*, 4081. [[CrossRef](#)] [[PubMed](#)]
5. Curry, S.; Brick, P.; Franks, N.P. Fatty acid binding to human serum albumin: New insights from crystallographic studies. *Biochim. Biophys. Acta* **1999**, *1441*, 131–140. [[CrossRef](#)] [[PubMed](#)]
6. Bhattacharya, A.A.; Grüne, T.; Curry, S. Crystallographic analysis reveals common modes of binding of medium and long-chain fatty acids to human serum albumin. *J. Mol. Biol.* **2000**, *303*, 721–732. [[CrossRef](#)]
7. Petitpas, I.; Grüne, T.; Bhattacharya, A.A.; Curry, S. Crystal structures of human serum albumin complexed with monounsaturated and polyunsaturated fatty acids. *J. Mol. Biol.* **2001**, *314*, 955–960. [[CrossRef](#)]
8. Petitpas, I.; Bhattacharya, A.A.; Twine, S.; East, M.; Curry, S. Crystal structure analysis of warfarin binding to human serum albumin anatomy of drug site I. *J. Biol. Chem.* **2001**, *276*, 22804–22809. [[CrossRef](#)]
9. Sudlow, G.; Birkett, D.J.; Wade, D.N. Further characterization of specific drug binding sites on human serum albumin. *Mol. Pharmacol.* **1976**, *12*, 1052–1061.
10. Krenzel, E.S.; Chen, Z.; Hamilton, J.A. Correspondence of fatty acid and drug binding sites on human serum albumin: A two-dimensional nuclear magnetic resonance study. *Biochemistry* **2013**, *52*, 1559–1567. [[CrossRef](#)]
11. Itoh, T.; Saura, Y.; Tsuda, Y.; Yamada, H. Stereoselectivity and enantiomer–enantiomer interactions in the binding of ibuprofen to human serum albumin. *Chirality* **1997**, *9*, 643–649. [[CrossRef](#)]
12. Murray, C.W.; Hartshorn, M.J. New applications for structure-based drug design. In *Comprehensive Medicinal Chemistry II*; Elsevier: Amsterdam, The Netherlands, 2007; Volume 4, Chapter 4.31; pp. 775–806.

13. Alexandri, E.; Primikyri, A.; Papamokos, G.; Venianakis, T.; Gkalpinos, V.G.; Tzakos, A.G.; Karydis-Messinis, A.; Moschovas, D.; Avgeropoulos, A.; Gerothanassis, I.P. NMR and computational studies reveal novel aspects in molecular recognition of unsaturated fatty acids with non-labeled serum albumin. *FEBS J.* **2022**, *289*, 5617–5636. [[CrossRef](#)] [[PubMed](#)]
14. Hernychova, L.; Alexandri, E.; Tzakos, A.G.; Zatloukalova, M.; Primikyri, A.; Gerothanassis, I.P.; Uhrík, L.; Šebela, M.; Kopečný, D.; Jedinák, L. Serum albumin as a primary non-covalent binding protein for nitro-oleic acid. *Int. J. Biol. Macromol.* **2022**, *203*, 116–129. [[CrossRef](#)] [[PubMed](#)]
15. Alexandri, E.; Venianakis, T.; Primikyri, A.; Papamokos, G.; Gerothanassis, I.P. Molecular basis for the selectivity of DHA and EPA in Sudlow's drug binding sites in human serum albumin with the combined use of NMR and docking calculations. *Molecules* **2023**, *28*, 3724. [[CrossRef](#)] [[PubMed](#)]
16. Gerothanassis, I.P. Ligand-observed in-tube NMR in natural products research: A review on enzymatic biotransformations, and in-cell NMR spectroscopy. *Arab. J. Chem.* **2023**, *16*, 104536. [[CrossRef](#)]
17. Wenskowsky, L.; Schreuder, H.; Derdau, V.; Matter, H.; Volkmar, J.; Nazaré, M.; Opatz, T.; Petry, S. Identification and characterization of a single high-affinity fatty acid binding site in human serum albumin. *Angew. Chem. Int. Ed.* **2018**, *57*, 1044–1048. [[CrossRef](#)] [[PubMed](#)]
18. He, X.M.; Carter, D.C. Atomic structure and chemistry of human serum albumin. *Nature* **1992**, *358*, 209–215. [[CrossRef](#)] [[PubMed](#)]
19. Claasen, B.; Axmann, M.; Meinecke, R.; Meyer, B. Direct observation of ligand binding to membrane proteins in living cells by a saturation transfer double difference (STDD) NMR spectroscopy method shows a significantly higher affinity of integrin  $\alpha(\text{IIb})\beta 3$  in native platelets than in liposomes. *J. Am. Chem. Soc.* **2005**, *127*, 916–919. [[CrossRef](#)] [[PubMed](#)]
20. Monaco, S.; Tailford, L.E.; Juge, N.; Angulo, J. Differential epitope mapping by STD NMR spectroscopy to reveal the nature of protein-ligand contacts. *Angew. Chem. Int. Ed.* **2017**, *56*, 15289–15293. [[CrossRef](#)]
21. Monaco, S.; Ramírez-Cárdenas, J.; Carmona, A.T.; Robina, I.; Angulo, J. Inter-ligand STD NMR: An efficient 1D NMR approach to probe relative orientation of ligands in a multi-subsite protein binding pocket. *Pharmaceuticals* **2022**, *15*, 1030. [[CrossRef](#)]
22. Potenza, D.; Vasile, F.; Belvisi, L.; Civera, M.; Araldi, E.M. STD and tr-NOESY NMR study of receptor-ligand interactions in living cancer cells. *Chem. Bio. Chem.* **2011**, *12*, 695–699. [[CrossRef](#)]
23. Mari, S.; Invernizzi, C.; Spitaleri, A.; Alberici, L.; Ghitti, M.; Bordignon, C.; Traversari, C.; Rizzardi, G.-P.; Musco, G. 2D Tr-NOESY experiments interrogate and rank ligand-receptor interactions in living human cancer cells. *Angew. Chem. Int. Ed.* **2010**, *49*, 1071–1074. [[CrossRef](#)]
24. Primikyri, A.; Sayyad, N.; Quilici, G.; Vrettos, E.I.; Lim, K.; Chi, S.-W.; Musco, G.; Gerothanassis, I.P.; Tzakos, A.G. Probing the interaction of a quercetin bioconjugate with Bcl-2 in living human cancer cells with in-cell NMR spectroscopy. *FEBS Lett.* **2018**, *592*, 3367–3379. [[CrossRef](#)] [[PubMed](#)]
25. Sanchez-Pedregal, V.M.; Reese, M.; Meiler, J.; Bloomers, M.J.J.; Griesinger, C.; Carlomagno, T. The INPHARMA method: Protein-mediated interligand NOEs for pharmacophore mapping. *Angew. Chem. Int. Ed.* **2005**, *44*, 4172–4175. [[CrossRef](#)] [[PubMed](#)]
26. Carlomagno, T. NMR in natural products: Understanding conformation, configuration and receptor interactions. *Nat. Prod. Rep.* **2012**, *29*, 536–554. [[CrossRef](#)]
27. Primikyri, A.; Papamokos, G.; Venianakis, T.; Sakka, M.; Kontogianni, V.; Gerothanassis, I.P. Structural basis of artemisinin binding sites in serum albumin with the combined use of NMR and docking calculations. *Molecules* **2022**, *27*, 5912. [[CrossRef](#)] [[PubMed](#)]
28. Kitchen, D.B.; Decornez, H.; Furr, J.R.; Bajorath, J. Docking and scoring in virtual screening for drug discovery: Methods and applications. *Nat. Rev. Drug Discov.* **2004**, *3*, 935–949. [[CrossRef](#)] [[PubMed](#)]
29. Morris, G.M.; Huey, R.; Lindstrom, W.; Sanner, M.F.; Belew, R.K.; Goodsell, D.S.; Olson, A.J. AutoDock4 and AutoDockTools4: Automated docking with selective receptor flexibility. *J. Comput. Chem.* **2009**, *30*, 2785–2791. [[CrossRef](#)] [[PubMed](#)]
30. Trott, O.; Olson, A.J. AutoDock Vina: Improving the speed and accuracy of docking with a new scoring function, efficient optimization, and multithreading. *J. Comput. Chem.* **2010**, *31*, 455–461. [[CrossRef](#)] [[PubMed](#)]
31. Meng, X.-Y.; Zhang, H.-X.; Mezei, M.; Cui, M. Molecular docking: A powerful approach for structure-based drug discovery. *Curr. Comput. Aided Drug Des.* **2011**, *7*, 146–157. [[CrossRef](#)]
32. Fehske, K.J.; Schäfer, U.; Wollert, U.; Müller, W.E. Characterization of an important drug binding area on human serum albumin including the high-affinity binding sites of warfarin and azapropazone. *Mol. Pharmacol.* **1982**, *21*, 387–393.
33. Kragh-Hansen, U. Evidence for a large and flexible region of human serum albumin possessing high affinity binding sites for salicylate, warfarin, and other ligands. *Mol. Pharmacol.* **1988**, *34*, 160–171.
34. Rafols, C.; Amezqueta, S.; Fuguet, E.; Bosch, E. Molecular interactions between warfarin and human (HSA) or bovine (BSA) serum albumin evaluated by isothermal titration calorimetry (ITC), fluorescence spectrometry (FS) and frontal analysis capillary electrophoresis (FA/CE). *J. Pharm. Biomed. Anal.* **2018**, *150*, 452–459. [[CrossRef](#)] [[PubMed](#)]
35. Rizzuti, B.; Bartucci, R.; Pey, A.L.; Guzzi, R. Warfarin increases thermal resistance of albumin through stabilization of the protein lobe that includes its binding site. *Arch. Biochem. Biophys.* **2019**, *676*, 10813. [[CrossRef](#)] [[PubMed](#)]
36. Cox, P.B.; Gupta, R. Contemporary computational applications and tools in drug discovery. *ACS Med. Chem. Lett.* **2022**, *13*, 1016–1029. [[CrossRef](#)] [[PubMed](#)]
37. Feher, M.; Williams, C.I. Effect of input differences on the results of docking calculations. *J. Chem. Inf. Model.* **2009**, *49*, 1704–1714. [[CrossRef](#)] [[PubMed](#)]

38. Moitessier, N.; Englebienne, P.; Lee, D.; Lawandi, J.; Corbeil, C.R. Towards the development of universal, fast and highly accurate docking/scoring methods: A long way to go. *Brit. J. Pharmacol.* **2008**, *153*, S7–S26. [[CrossRef](#)]
39. Schaduangrat, N.; Lampa, S.; Simeon, S.; Gleeson, M.P.; Spjuth, O.; Nantasenamat, C. Towards reproducible computational drug discovery. *J. Cheminform.* **2020**, *12*, 9. [[CrossRef](#)]
40. Koehler Leman, J.; Lyskov, S.; Lewis, S.M.; Adolf-Bryfogle, J.; Alford, R.F.; Barlow, K.; Ben-Aharon, Z.; Farrell, D.; Fell, J.; Hansen, W.A. Ensuring scientific reproducibility in bio-macromolecular modeling via extensive, automated benchmarks. *Nat. Commun.* **2021**, *12*, 6947. [[CrossRef](#)]
41. Gentile, F.; Agrawal, V.; Hsing, M.; Ton, A.-T.; Ban, F.; Norinder, U.; Gleave, M.E.; Cherkasov, A. Deep Docking: A deep learning platform for augmentation of structure-based drug discovery. *ACS Cent. Sci.* **2020**, *6*, 939–949. [[CrossRef](#)]
42. Papamokos, G.V. The nature of the biological material and the irreproducibility problem in biomedical research. *EMBO J.* **2019**, *38*, e101011. [[CrossRef](#)]
43. Ghuman, J.; Zunszain, P.A.; Petitpas, I.; Bhattacharya, A.A.; Otagiri, M.; Curry, S. Structural basis of the drug-binding specificity of human serum albumin. *J. Mol. Biol.* **2005**, *353*, 38–52. [[CrossRef](#)] [[PubMed](#)]
44. Fasano, M.; Curry, S.; Terreno, E.; Galliano, M.; Fanali, G.; Narciso, P.; Notari, S.; Ascenzi, P. The extraordinary ligand binding properties of human serum albumin. *IUBMB Life* **2005**, *57*, 787–796. [[CrossRef](#)] [[PubMed](#)]
45. Vaid, T.M.; Wu, F.-J.; Chalmers, D.K.; Scott, D.J.; Gooley, P.R. INPHARMA-based determination of ligand binding modes at  $\alpha_1$ -adrenergic receptors explains the molecular basis of subtype selectivity. *Chem. Eur. J.* **2020**, *26*, 11796–11805. [[CrossRef](#)] [[PubMed](#)]

**Disclaimer/Publisher’s Note:** The statements, opinions and data contained in all publications are solely those of the individual author(s) and contributor(s) and not of MDPI and/or the editor(s). MDPI and/or the editor(s) disclaim responsibility for any injury to people or property resulting from any ideas, methods, instructions or products referred to in the content.